 ©2011 Kvantovaya Elektronika and Turpion Ltd

PACS numbers: 07.60.Vg; 07.60.Ly; 07.79.Fc
DOI: 10.1070/QE2011v041n03ABEH014482

# Fibre Fabry – Perot cavity-based aperture probe for near-field optical microscopy systems

Yu.N. Kulchin, O.B. Vitrik, A.V. Bezverbnyi, E.V. Pustovalov,
A.A. Kuchmizhak, A.V. Nepomnyashchii

***Abstract*. We report a theoretical analysis and experimental study of the possibility of producing a novel type of interferometric near-field aperture probe for near-field optical microscopy systems using a fibre Fabry – Perot microcavity with a nanometre-scale aperture made in one of its output mirrors. The probe ensures a spatial resolution no worse than $\lambda/14$.**

***Keywords***: *aperture-based near-field optical microscopy, optical fibre Fabry – Perot interferometer, finite-difference time-domain method.*

High-resolution imaging of surface topography in nanostructured systems has always been a priority issue in micro- and nanoelectronics, microbiology and other areas of research. Scanning near-field optical microscopy (SNOM) is currently among the most attractive and effective techniques for imaging objects whose size cannot be determined by classical optical methods because of the fundamental diffraction limit. State-of-the-art SNOM systems are inferior in resolving power to scanning probe imaging techniques based on nonradiation fields (atomic force and scanning tunnelling microscopies) but require no vacuum for operation. Such systems enable subwavelength-resolution optical imaging of nanometre-scale systems [1] and basic research on the local spectroscopy of microbiological systems [1, 2] and semiconductor structures (quantum dots, wells, wires and others) [3] and on surface structure modification for ultra-high density information storage with a spatial resolution under 100 nm [4].

In the most widespread SNOM technique, a photodetector measures the intensity of a light beam passed through a scanning aperture probe and scattered by surface microroughness [1]. The probe typically has the form of a metal-coated silica core optical fibre strongly tapered towards its output end. The diffraction limit of optical systems can then be overcome by localising some of the light in the form of a nonpropagating (evanescent) field in the vicinity of a subwavelength aperture at the probe output end. The aperture diameter, which determines the resolving power of the SNOM system, is typically at least $\lambda/10$, where $\lambda$ is the wavelength of the light. Otherwise, the optical power decay in the evanescent part of the waveguide is too rapid, and photodetector sensitivity is insufficient for resolving small variations in the intensity of the light scattered by surface microroughness [5]. Thus, the insufficient sensitivity of the method under consideration limits the minimum aperture size and, accordingly, the spatial resolution of aperture SNOM systems.

It is known that the use of interferometric instead of amplitude principles markedly improves the sensitivity of measuring systems [6]. It is therefore reasonable to improve the sensitivity and, as a consequence, the resolving power of aperture SNOM techniques by measuring the probe radiation phase change resulting from the interaction between the evanescent field and the sample. One of the most sensitive types of interferometers, capable of detecting extremely small optical radiation phase changes, is the Fabry – Perot interferometer. In connection with this, the purpose of this work is to examine the possibility of using an optical fibre Fabry – Perot interferometer based aperture probe in SNOM systems.

We consider a probe in the form of a Fabry – Perot interferometer (Fig. 1a) with a cavity (*1*) formed by a section of bilayer step-index fibre and mirror coatings (*2*, *3*) on its end faces. One of the mirrors has a nanometre-scale aperture (*4*), which acts as a subwavelength-scale light source. The basic assumption behind the use of such a probe is that the phase change in the interferometer cavity as a result of the interaction of the optical field localised at the aperture output with the sample (*5*) shifts the resonance frequencies of the Fabry – Perot interferometer, and the shift can be used to evaluate the aperture – sample distance.

This assumption was verified by solving Maxwell's equations [7] using the finite-difference time-domain (FDTD) method, which has already been demonstrated to be an effective tool for assessing electromagnetic field parameters in optical media inhomogeneous on a subwavelength scale, including aperture probes [8].

The computations were performed for an optical fibre composed of a core with a refractive index $n_1 = 1.47$ and diameter $d_{\text{core}} = 8$ μm and a cladding of infinite diameter with a refractive index $n_2 = 1.465$. This model adequately describes the optical properties of standard weakly guiding fibres [9]. Because of the low core-cladding index contrast in

**Yu.N. Kulchin, O.B. Vitrik, A.V. Bezverbnyi, A.A. Kuchmizhak, A.V. Nepomnyashchii** Institute for Automation and Control Processes, Far Eastern Branch, Russian Academy of Sciences, ul. Radio 5, 690004 Vladivostok, Russia; e-mail: kulchin@iacp.dvo.ru;
**E.V. Pustovalov** Institute of Physics and Information Technologies, Far Eastern Federal University, ul. Sukhanova 8, 690950 Vladivostok, Russia; e-mail: pust@lemoi.phys.dvgu.ru

Received 18 November 2010
*Kvantovaya Elektronika* **41** (3) 249 – 252 (2011)
Translated by O.M. Tsarev

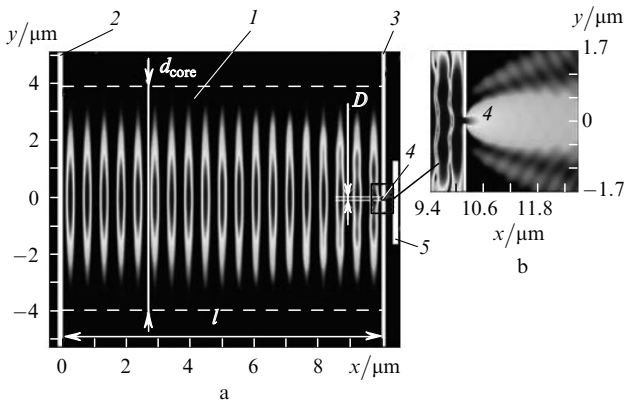


**Figure 1.** (a) Schematic of a fibre Fabry–Perot cavity with a nanometre-scale aperture: (*1z*) optical waveguide; (*2*, *3*) cavity mirrors; (*4*) output aperture; (*5*) sample. Electric field distributions (contours of constant $E_z$) (a) in the cavity and (b) near the output aperture (of width $D = \lambda/15$).

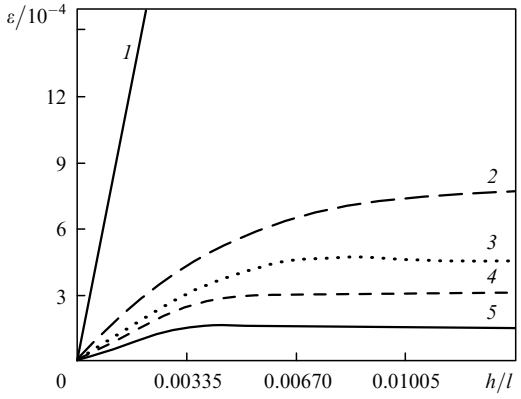


**Figure 2.** Relative change in resonance wavelength, $\varepsilon = \delta\lambda/\lambda$, as a function of $h/l$ at an aperture width $D = (1)\ 5\lambda$, $(2)\ \lambda/4$, $(3)\ \lambda/8$, $(4)\ \lambda/15$ and $(5)\ \lambda/40$.

this model, the transverse electric field component $E_z$ of an electromagnetic wave and its derivative $\partial E_z/\partial z$ can be considered continuous across the core–cladding interface [9]. The centre wavelength, $\lambda$, of the broadband light source is taken to be 1.55 μm, with a bandwidth $\Delta\lambda = 0.15$ μm, which implies that a single transverse mode is excited in the core. The mirrors of the plane-parallel cavity have the form of thin gold films. Their frequency-dependent electrical conductivity is assumed to follow Drude–Lorentz model predictions [10]. The sample, located distance $h$ from the aperture, is taken to have a smooth surface and to be an ideal electrical conductor, so that the electric field component $E_z$ is zero on its surface.

To simplify calculations and ensure stability of the modelling algorithm, we considered the simplest case of an extremely short plane-parallel optical cavity ($l = 20$ μm) based on a planar three-layer optical waveguide with a slit aperture at its output. In our experiments, we employed a probe in the form of a (cylindrical) fibre whose length exceeded that in the calculations. Nevertheless, the model used provides insight into the behaviour of the resonance frequencies of the interferometer and enables the sensitivity of the method to be approximately estimated.

The computed steady-state $E_z$ distributions in the Fabry–Perot cavity and at the output of a subwavelength aperture at an aperture width $D = \lambda/15$ are presented in Fig. 1. As seen, the field extends beyond the subwavelength aperture in the output mirror and interacts with the sample, converting to propagating radiation [1]. This changes the resonance frequencies of the interferometer in comparison with the $h = 0$ configuration. Figure 2 shows a family of curves that represent the computed relative change in the resonance wavelength of the interferometer, $\varepsilon = \delta\lambda/\lambda$, for various aperture sizes.

It follows from the computation results that the change in the resonance wavelength of the interferometer is governed by the $h/l$ ratio. When the aperture width approaches the core diameter, $\varepsilon$ is a linear function of $h/l$ [line (*1*)]. The reason for this behaviour is that a broad aperture has little or no effect on the spatial distribution of modes in the cavity, which are concentrated in the core. The cavity (Fig. 1a) is then defined by the input mirror of the interferometer (*2*) and the sample (*5*), and varying the sample position changes only the cavity length. This model is amenable to simple analytical treatment [6], which gives $\varepsilon = h/(n_1 l)$, in full accord with the computation results.

At subwavelength aperture widths, $\varepsilon$ is only proportional to $h/l$ at small $h$, comparable to the aperture size [Fig. 2, curves (*2–5*)], by virtue of evanescent to radiation mode conversion. With increasing $h$, the slope of the $\varepsilon(h/l)$ curves gradually decreases, approaching zero for $h \gg D$, where the sample is beyond the evanescent mode localisation region. The slope of the linear portion in the $\varepsilon(h/l)$ curves, $\alpha = l \times (n_1/\lambda)(\delta\lambda/h)$, which determines the sensitivity of the probe to the longitudinal displacement of the sample in the zone of the subwavelength aperture, varies from 0.7 for wide apertures [line (*1*)] to 0.07 at $D = \lambda/40$ [curve (*5*)].

The use of ideal conductors as mirrors of the Fabry–Perot cavity implies the maximum possible contrast of the interference pattern. An aperture of width $D \ll \lambda$ in one of the mirrors does not broaden the interference maxima, as supported by computation results. Under such conditions, even a minute change in resonance wavelength can in principle be detected. Real mirrors have reflectivities $r < 100\,\%$. According to the Rayleigh criterion [6], this limits the minimum resolvable shift of the resonance maximum, $\delta\lambda_{\min}$, of the interferometer. Based on this criterion, it is easy to show that the longitudinal resolution of the proposed method is $h_{\min} = n_1 l(\alpha Q)^{-1}$, where $Q = 2\pi l(n_1/\lambda) \times \sqrt{r}/(1-r)$ is the cavity finesse at zero absorption loss. It follows from the above that, at an aperture width $D = \lambda/15$, the sensitivity of the probe is quite sufficient to ensure a longitudinal resolution in the order of the subwavelength aperture size if the reflectivities of the cavity mirrors exceed 93 %. Such reflectivities are easy to reach in experiments, even by using thin-film metallic mirrors.

To verify the numerical modelling results, we designed a prototype near-field optical probe based on a fibre Fabry–Perot cavity. The probe had the form of a section of standard bilayer fibre ($l = 7$ mm, $d_{\text{core}} = 8$ μm, $n_1 = 1.473$, $n_2 = 1.4677$) with thin metallic films grown on its end faces by ion-beam sputtering.

The thickness of the films, $d$, was adjusted so as to reach a high cavity finesse, which can be ensured by increasing the reflectivity of the mirrors, $r$, and, hence, the thickness of the reflective coatings. In addition, the output mirror should be thick enough to prevent the light from passing through the coating beyond the subwavelength aperture, which other-

wise may lead to misinterpretation of the shift of resonance maxima. Too thick a coating may lead to an increase in power loss in the cavity and, hence, may limit the sensitivity of the method. As a trade-off, the film thickness on the input face of the waveguide was $d_1 = 45$ nm ($r_1 = 80\,\%$), and the film on the output face was slightly thicker: $d_2 = 60$ nm ($r_2 = 98\,\%$). According to our experiments, this solution ensures a finesse $Q \sim 0.5 \times 10^5$, sufficient to detect small changes in the resonance wavelengths of the fibre cavity, and rules out radiation–sample interaction beyond the subwavelength aperture.

Subwavelength apertures of various shapes (Fig. 3) can be made in output mirrors by ion beam etching (Carl Zeiss CrossBeam 1540-ESB). The shape of the aperture in Fig. 3a approaches the circular shape of the output hole of a standard aperture probe, which would be expected to ensure identical spatial resolutions when a sample will be scanned along two coordinate axes. The electron micrograph in Fig. 3a demonstrates however that the aperture deviates from the ideal circular shape, which was caused by technical problems. The slit aperture in Fig. 3b appears an optimal approach for scanning samples along one axis (centrosymmetric samples). Moreover, this shape fits in better with the numerical model under consideration.

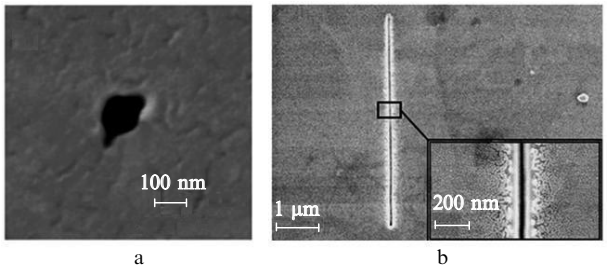


**Figure 3.** Electron micrographs of (a) a circular aperture of diameter $D = \lambda/15$ and (b) a slit aperture of width $D = \lambda/40$, both produced by ion beam etching.

The effect of aperture–sample distance on the resonance frequency of the Fabry–Perot interferometer was studied experimentally using the setup shown schematically in Fig. 4. Technical problems prevented us from producing an aperture less than 100 nm in size, but the use of a light emitting diode with a sufficiently long centre wavelength, $\lambda = 1553$ nm, ensured a large $\lambda/D$ ratio. The test sample used was a tapered optical fibre (Fig. 4, inset A) with a tip's radius of curvature of $\sim 300$ nm. This radius is sufficiently large compared to $D$, so that when the sample is in a central position with respect to the aperture, its surface can be considered almost flat, as was assumed in the numerical modelling. On the other hand, the tip radius was small enough to estimate the resolution of the proposed SNOM technique. The sample was positioned and scanned near the aperture by an XYZ positioning system with a ca. 10-nm accuracy. In experiments with a slit aperture, the light polarisation direction was normal to the slit, as in our computations.

Figure 5 shows the experimentally determined relative change of the resonance wavelength of a Fabry–Perot interferometer as a function of probe–sample distance for circular [curve (*2*)] and slit [curve (*3*)] apertures. Since the cavity length in our experiments considerably exceeded

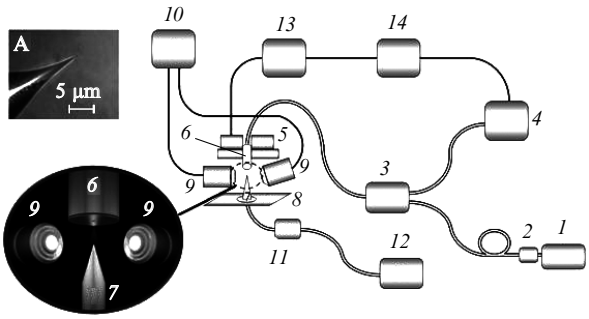


**Figure 4.** Schematic of the experimental setup: (*1*) light emitting diode; (*2*) polariser; (*3*) $2 \times 11$ fibre coupler; (*4*) fibre-optic spectrum analyser; (*5*, *8*) scanning systems; (*6*) optical fibre Fabry–Perot interferometer; (*7*) sample; (*9*) microscope objectives (magnification of $7000^{\times}$); (*10*) image processing system of a video microscope; (*11*) photodetector; (*12*) digital oscilloscope; (*13*) position control system of the scanning system; (*14*) computer. Inset A: optical micrograph of the sample tip.

that in the numerical simulation, the experimental data and computation results cannot be presented in one figure. Nevertheless, comparison of the data in Figs 2 and 5 demonstrates that the experimental curves are on the whole similar in shape to the calculated curves. At the same time, at a given value of $D$ the linear portion of the experimental curve is 2.5 times as steep as that of the calculated curve. The likely reason for this is that the experimental conditions differed from the model conditions.

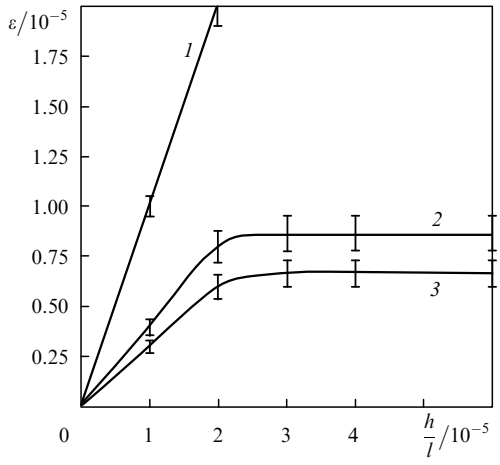


**Figure 5.** Relative shift of the resonance maximum of a Fabry–Perot interferometer, $\varepsilon$, as a function of $h/l$ for circular apertures of diameter $D = (1)\ \lambda$ and (*2*) $\lambda/15$ and (*3*) a slit aperture of width $D = \lambda/40$.

Figure 6 presents results for a sample tip scanned by a circular-aperture cavity along the $y$ axis at a constant height and a sample–aperture distance $h \sim 10$ nm. According to these data, the lateral resolution of the method, evaluated from the 10 % to 90 % edge response, is $\sim 120$ nm, which is roughly equal to the aperture diameter.

Thus, the present theoretical and experimental results suggest the possibility of producing a scanning aperture probe for aperture-based near-field optical microscopy using a fibre Fabry–Perot cavity. The proposed method ensures lateral and vertical resolutions within 120 nm, which corresponds to $\sim \lambda/14$ at $\lambda = 1550$ nm. The spatial reso-

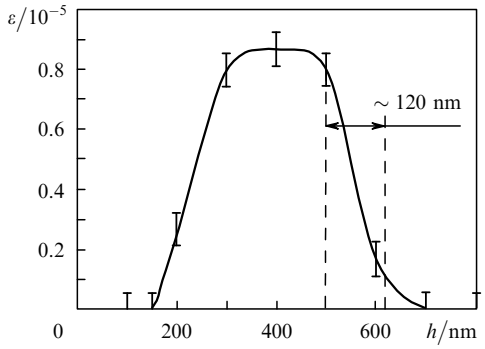


**Figure 6.** Relative shift of the resonance maximum, $\varepsilon$, as a function of $h$ for a sample tip scanned along the $y$ axis.

lution of the method can be further improved by taking advantage of higher finesse cavities.

## References

1. Hecht B., Sick fl., Wild U.P., et al. *J. Chem. Phys.*, **112**, 7761 (2000).
2. Nagahara L.A., Yanagi H., Tokumoto H. *Nanotechnology*, **8**, 50 (1997).
3. Matsuda K., Saiki T., Saito H., Nishi K. *Appl. Phys. Lett.*, **76**, 73 (2000).
4. Davis C.C., Atia W.A., Gungor A., Mazzoni D.L., Pilevar S. *Laser Phys.*, **7**, 243 (1997).
5. Novotny L., Hecht B. *Principles of Nano-Optics* (Cambridge: Cambridge University Press, 2006).
6. Born M., Wolf E. *Principles of Optics* (Oxford: Pergamon, 1969; Moscow: Nauka, 1973).
7. Taflove A., Hagness S.C. *Computational Electrodynamics: The Finite-Difference Time-Domain Method* (Boston, MA: Artech House, Inc., 2000).
8. Krug J.T., Sánchez E.J., Xie X.S. *J. Chem. Phys.*, **116**, 10895 (2002).
9. Snyder A.W., Love J.D. *Optical Waveguide Theory* (London: Chapman and Hall, 1983; Moscow: Radio i Svyaz', 1987).
10. Johnson P.B., Christy R.W. *Phys. Rev. B*, **6**, 4370 (1972).